Original Article

Improved Performance in Differentiating Benign from Malignant Sinonasal Tumors Using Diffusion-weighted Combined with Dynamic Contrast-enhanced Magnetic Resonance Imaging

Xin-Yan Wang[1], Fei Yan[1], Hui Hao[1], Jian-Xing Wu[1], Qing-Hua Chen[1], Jun-Fang Xian[1,2]

[1]Department of Radiology, Beijing Tongren Hospital, Capital Medical University, Beijing 100730, China

[2]Beijing Key Laboratory of Nasal Diseases, Beijing Institute of Otolaryngology, Capital Medical University, Beijing 100069, China

Abstract

Background: Differentiating benign from malignant sinonsal lesions is essential for treatment planning as well as determining the patient's prognosis, but the differentiation is often difficult in clinical practice. The study aimed to determine whether the combination of diffusion-weighted (DW) and dynamic contrast-enhanced magnetic resonance imaging (DCE-MRI) can improve the performance in differentiating benign from malignant sinonasal tumors.

Methods: This retrospective study included 197 consecutive patients with sinonasal tumors (116 malignant tumors and 81 benign tumors). All patients underwent both DW and DCE-MRI in a 3-T magnetic resonance scanner. Two different settings of b values (0,700 and 0,1000 s/mm^2) and two different strategies of region of interest (ROI) including whole slice (WS) and partial slice (PS) were used to calculate apparent diffusion coefficients (ADCs). A DW parameter with WS $ADCs_{b0,1000}$ and two DCE-MRI parameters (time intensity curve [TIC] and time to peak enhancement [Tpeak]) were finally combined to use in differentiating the benign from the malignant tumors in this study.

Results: The mean ADCs of malignant sinonasal tumors (WS $ADCs_{b0,1000} = 1.084 \times 10^{-3}$ mm^2/s) were significantly lower than those of benign tumors (WS $ADCs_{b0,1000} = 1.617 \times 10^{-3}$ mm^2/s, $P < 0.001$). The accuracy using WS $ADCs_{b0,1000}$ alone was 83.7% in differentiating the benign from the malignant tumors (85.3% sensitivity, 81.2% specificity, 86.4% positive predictive value [PPV], and 79.5% negative predictive value [NPV]). The accuracy using DCE with Tpeak and TIC alone was 72.1% (69.1% sensitivity, 74.1% specificity, 77.5% PPV, and 65.1% NPV). Using DW-MRI parameter was superior than using DCE parameters in differentiation between benign and malignant sinonasal tumors ($P < 0.001$). The accuracy was 87.3% (90.5% sensitivity, 82.7% specificity, 88.2% PPV, and 85.9% NPV) using DW-MRI combined with DCE-MRI, which was superior than that using DCE-MRI alone or using DW-MRI alone (both $P < 0.001$) in differentiating the benign from the malignant tumors.

Conclusions: Diffusion-weighted combined with DCE-MRI can improve imaging performance in differentiating benign from malignant sinonasal tumors, which has the potential to improve diagnostic accuracy and to provide added value in the management for these tumors.

Key words: Diffusion-weighted; Dynamic Contrast-enhanced; Magnetic Resonance Imaging; Nasal Cavity; Neoplasm; Paranasal Sinus

Introduction

The sinonasal area is affected by a wide spectrum of benign and malignant tumors and tumor like lesions. It is essential to distinguish benign from malignant sinonsal tumors for treatment planning as well as determining the patient's prognosis. However, the presenting symptoms of benign and malignant sinonasal tumors, such as nasal discharge, epistaxis and nasal obstruction are often nonspecific. Moreover, although endoscopic excisional biopsy in the sinonasal area is performed easily and used widely, the diagnostic sensitivity is low due to the fact that surrounding inflammatory tissues may be obtained.[1] Therefore, the effective differentiation between benign and malignant sinonasal tumors is often difficult in the clinical practice.

Conventional computed tomography (CT) and magnetic resonance imaging (MRI) play essential roles in the diagnosis of sinonasal lesions.[2-8] CT provides excellent details about the thin bony sinonasal walls, but is of limited value in characterization of soft tissue mass due to poor soft tissue contrast resolution. MRI is now widely accepted as the best technique for the characterization of an

Access this article online

Quick Response Code:

Website: www.cmj.org

DOI: 10.4103/0366-6999.151649

Address for correspondence: Dr. Jun-Fang Xian, Department of Radiology, Beijing Tongren Hospital, Capital Medical University, Beijing 100730, China
E-Mail: cjr.xianjunfang@vip.163.com

indeterminate mass due to the excellent soft tissue resolution, and many MRI features contribute a lot to the diagnosis of sinonasal tumors. Nevertheless, these MRI features are often nonspecific. For example, convoluted cerebriform pattern is a reliable MRI feature of sinonasal inverted papillomas,[8] but it is also demonstrated in a proportion of malignant tumors. Therefore, the discrimination between benign and malignant tumors on the basis of conventional CT and MRI findings is still difficult in a substantial number of cases,[9,10] and new imaging method is required to improve the discrimination.

Recent studies have demonstrated the utility of functional MRI techniques such as diffusion-weighted (DW) and dynamic contrast-enhanced (DCE) MRI in head and neck region, which offer better characterization of tissues and physiological processes in the diagnosis of tumors.[11-18] Apparent diffusion coefficients (ADCs) obtained from DW-MRI and time intensity curve (TIC) types obtained from DCE-MRI, have been shown to contribute to the diagnosis of head and neck tumors.[11-18] However, overlaps of ADCs and TIC types have been also shown between benign and malignant tumors in head and neck region including sinonasal region.[9,12,16] Therefore, the use of any single technique may not be effective enough. In this regard, combined use of DW-MRI and DCE-MRI have been tried in head and neck region and demonstrated to successfully improve the differentiation between benign and malignant tumors.[19,20] Similar studies have been also conducted in the sinonasal region,[21] but the study sample was small and more than half of the benign lesions in the study were inflammatory lesions, which showed extremely high ADCs. Therefore, in the present study, we tested whether the combined use of DW-MRI and DCE-MRI could provide effective differentiation between benign and malignant sinonasal tumors and tumor like lesions with a larger sample.

Methods

Patient data

The protocol of this retrospective study was approved by Institutional Review Board of Beijing Tongren Hospital, and informed consent was obtained from all patients. The DW-MRI and DCE-MRI were retrospectively analyzed in 197 patients (123 males and 74 females) with histologically proved sinonasal tumors and tumor like lesions, who received MR examinations from October 2011 to December 2013. The other inclusion criteria of the study required the following features: (1) the short-axis diameter of the mass >1 cm; (2) the mass was proved by histologic examination to be a malignant or benign tumor or tumor like lesion; (3) both DW-MRI and DCE-MRI were available; (4) no biopsy or treatment prior to MRI. The exclusion criteria were: (1) inflammatory lesions and recurrent tumors; (2) sinonasal angiomatous polyps were also excluded owing to the fact that it can be easily diagnosed by its characteristic features of MRI (a peripheral hypointense rim on T2-weighted image and progressive enhancement on DCE-MRI).[22]

Magnetic resonance imaging technique

MRI was performed with a 3-T MR imager (GE Healthcare, Milwaukee, Wisconsin, USA), using an 8-channel phased-array head coil. DW-MRI: axial DW images (DWI) (repetition time [TR]/echo time [TE]/number of signal intensity acquisitions, 4000 ms/75 ms/4) were obtained using duo periodically rotated overlapping parallel lines with enhanced reconstruction (PROPELLER) imaging. A 4 mm section thickness, a 0.5 mm intersection gap, a field of view (FOV) of 18 cm × 18 cm and a matrix of 128 × 128 were used. The total time was 2 minutes 16 seconds. We used two different settings of b values (0,700 and 0,1000 s/mm^2) to determine ADCs.

Dynamic contrast-enhanced-magnetic resonance imaging

Transverse DCE-MRI was obtained using a fast spoiled gradient recalled sequence, a flip angle of 15°, one excitation, a matrix of 256 × 160 and a slice thickness of 3.2 mm. The scan time for each patient was about 344 seconds, and in each patient, 37 scans were obtained at an interval of 0–2 seconds. Gadopentetate dimeglumine contrast agent (Magnevist; Bayer Schering, Berlin, Germany) was delivered intravenously (0.1 mmol/kg) at a flow rate of 2 ml/s using an automatic injector (Medrad, Indianola, Pennsylvania, USA). Conventional MRI: axial T1-weighted image, T2-weighted image and coronal T1-weighted image was obtained with fast spin echo sequences (T1-weighted image: TR 400–500 ms, TE 10 ms, matrix 320 × 256; T2-weighted image: TR 3500–4000 ms, TE 190 ms, matrix 512 × 256; number of excitation = 2, FOV = 18 cm × 18 cm; section thickness = 4–5 mm, intersection gap = 0.5 mm).

Imaging analysis

Image analysis was performed on a workstation (Advantage Workstation, AW 4.4, GE Medical Systems, Milwaukee, Wisconsin, USA). ADC measurements were performed using the following two different sampling strategies of the region of interests (ROIs): (1) a single DW-MRI obtained from the maximum area of each tumor was used. Freehand ROI (whole slice [WS]) were placed onto b = 0 image such that it encompassed as much of the tumor area as possible, avoiding any necrotic regions; (2) on the same slice, small ROIs about 30 mm^2 (partial slice [PS]) containing areas, where the ADC value was the lowest, was determined to calculate PS ADC.

For DCE-MRI analysis, a circular ROI with an area of 10 mm^2 that showed the most avidly and early enhancing solid component on the dynamic images was manually drawn. The following parameters were calculated: the time to peak enhancement (Tpeak), the time to maximum enhancement (Tmax) and maximum contrast index (CImax = signal intensity [max–contrast]–signal intensity [precontrast]/signal intensity [precontrast]). The TICs were referred to as persistent, plateau or washout-shaped curves.

Statistical analysis

Differences in ADCs and DCE-MRI parameters between benign and malignant sinonasal tumors were determined by

independent samples *t*-test and Chi-square test, respectively. A $P < 0.05$ was considered to be statistically significant. Multivariate logistic regression analysis was used to determine which model (model 1: DCE-MRI; model 2: DW-MRI; model 3: DW-MRI combined with DCE-MRI) was the best in differentiation between benign and malignant tumors. The statistical analyses were performed using SPSS 17.0 (SPSS, Chicago, IL, USA).

Results

Patients and diagnosis

The diagnosis of 81 benign tumors (57 males and 24 females; mean age, 45.11 ± 16.33 years) and 116 malignant tumors (66 males and 50 females; mean age, 49.06 ± 16.44 years) were shown in Table 1. There was no significant difference in age or sex of patients between benign and malignant sinonasal tumors, respectively ($P = 0.099$ and $P = 0.055$).

Differentiation between benign and malignant sinonasal tumors with diffusion-weighted-magnetic resonance imaging alone

The ADCs of malignant sinonasal tumors were significantly ($P < 0.001$) lower than those of benign tumors [Table 2 and Figures 1-4], and the performance of ADCs in the differentiation of benign and malignant tumors was shown in Table 3. The $ADCs_{b0,700}$ of sinonasal tumors were significantly higher than $ADCs_{b0,1000}$ (PS ADCs, $P < 0.001$; WS ADCs, $P < 0.001$), but there was no significant difference in the performance between $ADCs_{b0,700}$ and $ADCs_{b0,1000}$ (PS ADCs, $P = 0.689$; WS ADCs, $P = 0.741$). Additionally, PS ADCs of sinonasal tumors were significantly lower than WS ADCs ($ADCs_{b0,700}$, $P < 0.001$; $ADCs_{b0,1000}$, $P < 0.001$), but no significant difference was found in diagnostic ability between these two different ROI sampling strategies ($ADCs_{b0,700}$, $P = 0.578$; $ADCs_{b0,1000}$, $P = 0.561$).

Table 1: Diagnosis of 197 sinonasal tumors

Diagnosis of lesions	Number (*n*)	Percentage
Malignant tumors	116	100
Lymphoma	22	18.9
Adenoid cystic carcinoma	16	13.8
Malignant melanoma	11	9.5
SCC	11	9.5
Rhabdomyosarcoma	10	8.6
Inverted papilloma with malignant transformation	10	8.6
Olfactory neuroblastoma	9	7.8
Ewing's sarcoma	4	3.4
Adenocarcinoma	4	3.4
Primitive neuroectodermal tumor	2	1.7
Plasmacytoma	2	1.7
Osteosarcoma	2	1.7
Metastasis of renal carcinoma	2	1.7
Undifferentiated carcinoma	2	1.7
Other	9	7.8
Benign tumors	81	100
Inverted papilloma	48	59.3
Hemangioma	9	11.1
Schwannoma	5	6.2
Ossifying fibroma	4	4.9
Fibroangioma	4	4.9
Ameloblastoma	2	2.5
Hemangiopericytoma	2	2.5
Other	7	8.6

SCC: Squamous cell carcinoma.

Differentiation between benign and malignant sinonasal tumors with dynamic contrast-enhanced magnetic resonance imaging alone

Dynamic contrast-enhanced-MRI parameters of benign and malignant sinonasal tumors were demonstrated in Table 4. Cut-off points for Tpeak (76.5 seconds), Tmax (143.5 seconds), and a washout-shaped TIC differentiated benign from malignant sinonasal tumors with an accuracy of 71.0%, 70.6% and 71.1%, respectively [Table 5].

Differentiation between benign and malignant sinonasal tumors with combination of diffusion-weighted and dynamic contrast-enhanced magnetic resonance imaging

Diagnostic abilities of different MRI methods were described in Table 6. The logistic regression model 3, based on the

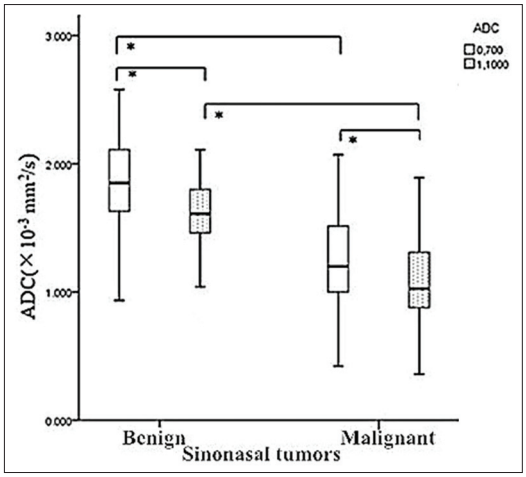

Figure 1: Whole slice (WS) apparent diffusion coefficients $(ADCs)_{b0,700}$ and $ADCs_{b0,1000}$ of benign and malignant sinonasal tumors were demonstrated in the graph (box plots). WS ADCs of malignancy were lower than those of benign tumors, and $ADCs_{b0,700}$ were significantly higher than $ADCs_{b0,1000}$ (*$P < 0.001$).

Table 2: Mean ADCs of benign and malignant sinonasal tumors

ROI	b values	ADC value (×10⁻³ mm²/s)		*P*
		Malignant (*n* = 116)	Benign (*n* = 81)	
WS	0,700	1.259 ± 0.361	1.892 ± 0.332	<0.001
WS	0,1000	1.084 ± 0.317	1.659 ± 0.281	<0.001
PS	0,700	1.068 ± 0.340	1.637 ± 0.273	<0.001
PS	0,1000	0.924 ± 0.294	1.436 ± 0.241	<0.001

ROI: Region of interest; WS: Whole slice; PS: Partial slice; ADC: Apparent diffusion coefficient.

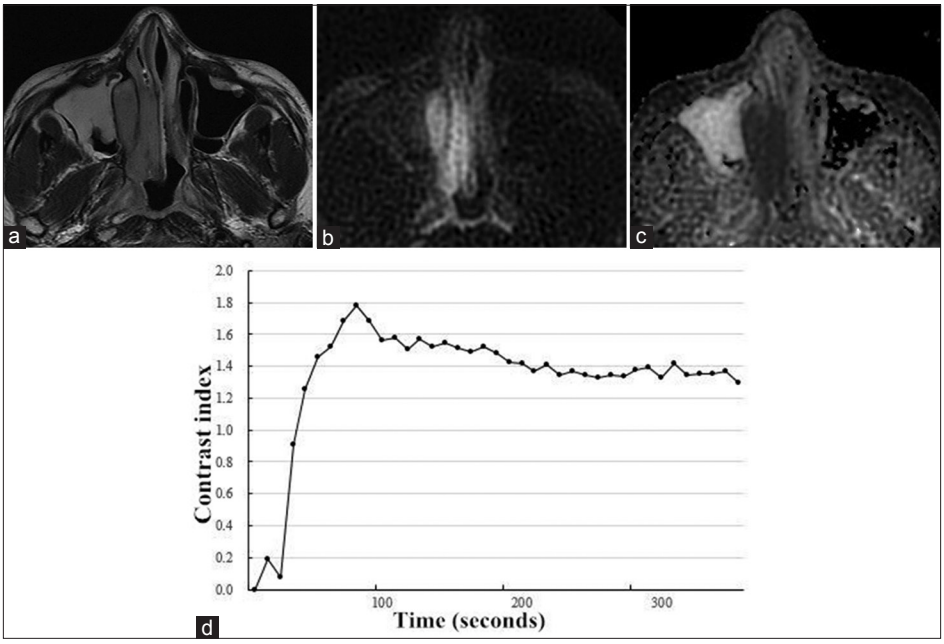

Figure 2: Magnetic resonance images (MRI) of a 28-year-old man with NK/T-cell lymphoma in right nasal cavity. (a) Axial T2-weighted MRI demonstrated a homogeneously isointense mass in right nasal cavity. (b) The mass showed hyperintense on transverse diffusion-weighted imaging at b = 1000 s/mm^2. (c) On axial apparent diffusion coefficient (ADC) map at b = 0,1000 s/mm^2, the mass appeared low signal intensity with whole slice $ADC_{b0,1000}$ = 0.803 × 10^{-3} mm^2/s, suggesting a malignant tumor. (d) Time-intensity curve was characterized as a washout curve.

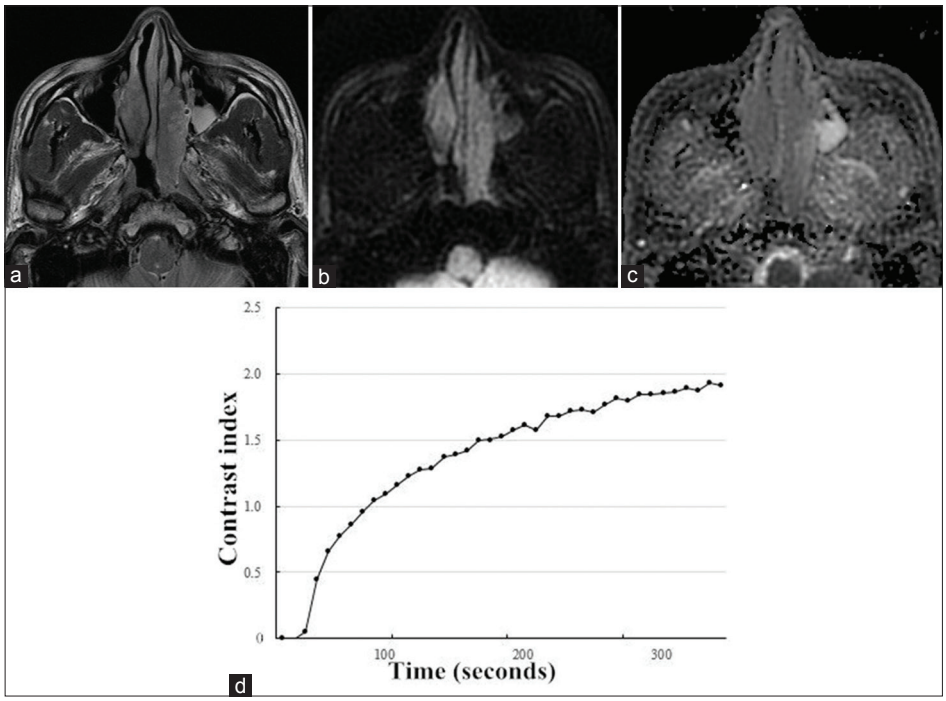

Figure 3: A 49-year-old man with inverted papilloma in the left nasal cavity. (a) Axial T2-weighted magnetic resonance image showed a mass with heterogeneously intermediate signal intensity. (b) The mass appeared hypointense on transverse diffusion-weighted imaging at b = 1000 s/mm^2. (c) Corresponding apparent diffusion coefficient (ADC) map demonstrated hyperintense mass with whole slice $ADC_{b0,1000}$ = 1.610 × 10^{-3} mm^2/s. (d) Time-intensity curve in this patient was characterized as a persistent curve.

combined use of DW-MRI and DCE-MRI, was superior to DCE-MRI ($P < 0.001$) and DW-MRI ($P < 0.001$) alone in discriminating benign from malignant tumors in the sinonasal region. The best MRI parameters of model 3 in discriminating benign from malignant tumors were Tpeak (odds ratio [*OR*] = 3.419, 95% confidence interval [*CI*] 1.184–9.875), WS $ADCs_{b0,1000}$ (*OR* = 0.005, 95% *CI* (0.001–0.021) and washout-type TIC (*OR* = 4.215, 95% *CI* 1.924–9.234).

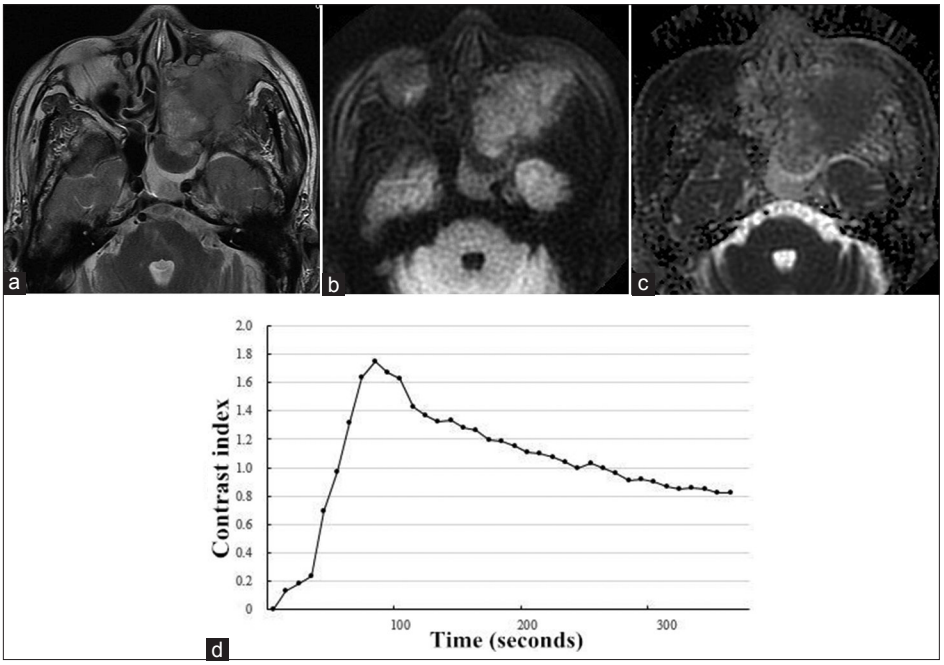

Figure 4: (a) Axial T2-weighted magnetic resonance image in a 76-year-old man showed a left-sided tumor mass in the maxillary and ethmoid sinus with heterogeneously intermediate signal intensity. (b) On axial diffusion-weighted imaging at b = 1000 s/mm^2, the mass showed limited signal loss. (c) Corresponding apparent diffusion coefficient (ADC) map showed the mass with whole slice $ADC_{b0,1000}$ = 1.170 × 10^{-3} mm^2/s. (d) Time-intensity curve in this patient was characterized as a washout-shaped pattern.

Table 3: The performance of ADCs in differentiation between benign and malignant sinonasal tumors

ROI	b values	Threshold of ADCs (×10^{-3} mm^2/s)	Sensitivity (%)	Specificity (%)	PPV (%)	NPV (%)	Accuracy (%)
WS	0,700	1.615	80.2	87.7	90.3	75.5	83.2
WS	0,1000	1.370	85.3	81.2	86.4	79.5	83.7
PS	0,700	1.245	68.1	93.7	94.0	67.3	78.7
PS	0,1000	1.175	78.4	82.2	86.7	72.8	80.2

ROI: Region of interest; WS: Whole slice; PS: Partial slice; PPV: Positive predictive value; NPV: Negative predictive value; ADC: Apparent diffusion coefficient.

Discussion

Sinonasal tumors consist of a large number of benign and malignant tumors.[2-5] The malignant sinonasal tumors, a variety of histological types mainly including squamous cell carcinoma, adenoid cystic carcinoma and lymphomas, can invade into the critical structures of the anterior and central skull base and threaten one's life.[3] Thus, distinguishing between benign and malignant sinonasal tumors is crucial for treatment planning as well as determining the patient's prognosis. However, despite imaging developments, effective diagnosis of sinonasal lesions only on the basis of conventional CT and MRI is still difficult. Many signs of malignant tumors are interpreted as rhinosinusitis or benign lesions.[2-5] Therefore, new imaging methods are required to improve the discrimination between benign and malignant tumors in sinonasal region.

DCE-MRI has been applied to differentiate between benign and malignant tumors in head and neck region.[14-18] It has been reported that DCE-MRI parameters, especially TIC, play important roles in the diagnosis of head and neck tumors including orbital, salivary gland and thyroid tumors.[14-18] However, few similar studies focused on sinonasal tumors.[21] Sasaki *et al*.[21] reported that significant overlaps in overall TICs were present between benign and malignant sinonasal tumors, but successful discrimination was achieved on pixel-by-pixel basis. Nevertheless, besides the small sample of their study (n = 44), pixel-by-pixel based TIC analysis was time-consuming and difficult to carry out in clinical practice. The present study showed that washout-shaped TICs discriminated the benign and malignant sinonasal tumors with an accuracy of 71.1%. The possible reason for the relatively low differentiating performance may be that a large number of vascular tumors including hemangiomas and fibroangiomas were included in the study, which also showed washout-shaped TIC as same as the malignant tumors.[23] Thus, differentiation between benign and malignant tumors based on DCE-MRI alone has the limitation for those tumors.

DW-MRI, which was used to quantify the diffusional motion of water with the ADC, has also been employed for diagnosing head and neck lesions.[11-13,24-26] Previous studies reported that ADCs were useful in discrimination not only between benign and malignant tumors but also between benign and metastatic lymphnodes in the head and neck

region.[13] For sinonasal tumors, a previous study showed effective differentiation between benign and malignant sinonasal lesions (93% accuracy) was achieved by ADCs.[27] Nevertheless, inflammatory polyps that showed extremely high ADCs were also included in the benign tumor group, which only consisted of 12 cases. Another study showed ADC mapping based on a pixel-by-pixel analysis of the whole tumor volume facilitated the differentiation between benign/inflammatory lesions and malignant tumors in the sinonasal area.[11] However, despite its promising results (85% accuracy), the ADC mapping based on a pixel-by-pixel analysis of the whole tumor volume may be difficult for routine clinical use. In our study, PROPELLER DWI was used to decrease distortion and severe artifacts, and two different b-value settings and sampling strategies of ROIs were compared. Based on our results, even though ADCs with different b-value settings and sampling strategies of ROIs were different, no significant difference in the performance was found between two strategies of ROIs or different b-value settings, consistent with the previous study which focused on differentiation between lymphomas and carcinomas.[28] However, performance in differentiating malignant and benign tumors using ADCs alone was still not very high (it was 83.7% in our study).

Given that the single use of either DCE-MRI parameters or ADCs was not effective enough for differentiating benign and malignant tumors, the combined use of DW-MRI and DCE-MRI has been employed in the head and neck region.[19,20] Previous studies reported that the combined use of DW-MRI and DCE-MRI improved the performance of head and neck tumors compared with the use of DW-MRI or DCE-MRI alone. Consistent with the previous findings, improved performance was also achieved by combination of ADCs and DCE-MRI parameters for sinonasal tumors in a large un-selected patient data set in our study. The comparison of performance between DCE-MRI parameter and ADCs was also performed in the present study and showed that performance of ADCs was significantly higher than that of DCE-MRI parameters. On the basis of this result, DW-MRI was recommended in patients with sinonasal tumors to increases the diagnostic accuracy, particularly for the patients who cannot undergo contrasted enhanced MRI because of an abnormality in renal function.

Table 4: Frequency distribution of DCE-MRI parameters of sinonasal tumors

DCE-MRI parameters	Types of lesions, *n* (%)			*P*
	Overall (*N* = 197)	Malignant (*n* = 116)	Benign (*n* = 81)	
Tpeak (seconds)				<0.001
T ≤ 60	91 (46.2)	70 (60.3)	21 (25.9)	
60 < T ≤ 80	36 (18.3)	21 (18.1)	15 (18.5)	
80 < T ≤ 100	18 (9.1)	12 (10.3)	6 (7.4)	
100 < T ≤ 120	18 (9.1)	4 (3.4)	14 (17.3)	
T > 120	34 (17.3)	9 (7.8)	25 (30.9)	
Tmax (seconds)				<0.001
T ≤ 60	40 (20.3)	33 (28.4)	7 (8.6)	
60 < T ≤ 80	24 (12.2)	17 (14.7)	7 (8.6)	
80 < T ≤ 100	20 (10.2)	15 (12.9)	5 (6.2)	
100 < T ≤ 120	19 (9.6)	13 (11.2)	6 (7.4)	
T > 120	94 (47.7)	38 (32.8)	56 (69.1)	
CImax				0.564
Contrast index ≤ 0.5	5 (2.5)	5 (4.3)	0 (0.0)	
0.5 < contrast index ≤ 1.0	61 (31.0)	34 (29.3)	27 (33.3)	
1.0 < contrast index ≤ 1.5	73 (37.1)	44 (37.9)	29 (35.8)	
Contrast index > 1.5	58 (29.4)	33 (28.4)	25 (30.9)	
TIC type				
Persistent	34 (17.3)	9 (7.8)	25 (30.9)	<0.001
Plateau-shaped	62 (31.5)	27 (23.3)	35 (43.2)	<0.001
Washout-shaped	101 (51.3)	80 (69.0)	21 (25.9)	<0.001

Tpeak: Time to peak enhancement; Tmax: Time to maximum enhancement; TIC: Time-intensity curve; DCE-MRI: Dynamic contrast-enhanced magnetic resonance imaging.

Table 5: The performance of DCE-MRI parameters in differentiation between benign and malignant sinonasal tumors

ROIs	Threshold of time (seconds)	Sensitivity (%)	Specificity (%)	PPV (%)	NPV (%)	Accuracy (%)
Tpeak	76.5	74.1	66.7	76.1	64.3	71.0
Tmax	143.5	76.7	61.7	74.2	64.9	70.6
Wash out TIC	–	69.0	74.1	79.2	62.5	71.1

Tpeak: Time to peak enhancement; Tmax: Time to maximum enhancement; TIC: Time-intensity curve; PPV: Positive predictive value; NPV: Negative predictive value; ROI: Region of interest; DCE-MRI: Dynamic contrast-enhanced magnetic resonance imaging.

Table 6: The performance of different MRI methods

Models	Parameters	Sensitivity (%)	Specificity (%)	PPV (%)	NPV (%)	Accuracy (%)
DCE-MRI	Tpeak and washout TIC	69.1	74.1	77.5	65.1	72.1
DWI-MRI	WS $ADCs_{b0,1000}$	85.3	81.2	86.4	79.5	83.7
DW-MRI combined with DCE MRI	Tpeak, Washout TIC and WS $ADCs_{b0,1000}$	90.5	82.7	88.2	85.9	87.3

Tpeak: Time to peak enhancement; PPV: Positive predictive value; NPV: Negative predictive value; WS: Whole slice; TIC: Time intensity curve; DCE-MRI: Dynamic contrast-enhanced magnetic resonance imaging; DWI-MRI: Diffusion-weighted imaging magnetic resonance imaging; MRI: Magnetic resonance imaging.

There are several limitations in our study. Firstly, the analysis of DWI was not based on the intravoxel incoherent motion imaging, which can quantitatively image both molecular diffusion of water and microcirculation of blood.[29] Secondly, the diagnostic accuracy provided by combined use of DW-MRI and DCE-MRI was still insufficient for preoperative differentiation between benign and malignant lesions. Thirdly, we did not show an analysis for the differentiating performance that was improved between different histological types of tumors in the sinonasal region, and we will submit it separately.

In conclusion, combination of ADCs and DCE-MRI parameters efficiently differentiated between benign and malignant sinonasal diseases. The findings suggested that a multiparametric approach using ADCs and DCE-MRI parameters differentiated between benign and malignant tumors, and the combination approach has the potential to improve diagnostic accuracy and to provide added value in patient management for these tumors.

References

1. Han MW, Lee BJ, Jang YJ, Chung YS. Clinical value of office-based endoscopic incisional biopsy in diagnosis of nasal cavity masses. Otolaryngol Head Neck Surg 2010;143:341-7.
2. Eggesbø HB. Imaging of sinonasal tumours. Cancer Imaging 2012;12:136-52.
3. Singh N, Eskander A, Huang SH, Curtin H, Bartlett E, Vescan A, *et al.* Imaging and resectability issues of sinonasal tumors. Expert Rev Anticancer Ther 2013;13:297-312.
4. Raghavan P, Phillips CD. Magnetic resonance imaging of sinonasal malignancies. Top Magn Reson Imaging 2007;18:259-67.
5. Loevner LA, Sonners AI. Imaging of neoplasms of the paranasal sinuses. Neuroimaging Clin N Am 2004;14:625-46.
6. Kim YS, Kim HJ, Kim CH, Kim J. CT and MR imaging findings of sinonasal schwannoma: a review of 12 cases. AJNR Am J Neuroradiol 2013;34:628-33.
7. Lee DG, Lee SK, Chang HW, Kim JY, Lee HJ, Lee SM, *et al.* CT features of lobular capillary hemangioma of the nasal cavity. AJNR Am J Neuroradiol 2010;31:749-54.
8. Maroldi R, Farina D, Palvarini L, Lombardi D, Tomenzoli D, Nicolai P. Magnetic resonance imaging findings of inverted papilloma: differential diagnosis with malignant sinonasal tumors. Am J Rhinol 2004;18:305-10.
9. Wang X, Zhang Z, Chen X, Li J, Xian J. Value of magnetic resonance imaging including dynamic contrast-enhanced magnetic resonance imaging in differentiation between inverted papilloma and malignant tumors in the nasal cavity. Chin Med J 2014;127:1696-701.
10. Maroldi R, Ravanelli M, Borghesi A, Farina D. Paranasal sinus imaging. Eur J Radiol 2008;66:372-86.
11. Sasaki M, Eida S, Sumi M, Nakamura T. Apparent diffusion coefficient mapping for sinonasal diseases: Differentiation of benign and malignant lesions. AJNR Am J Neuroradiol 2011;32:1100-6.
12. Thoeny HC, De Keyzer F, King AD. Diffusion-weighted MR imaging in the head and neck. Radiology 2012;263:19-32.
13. Barchetti F, Pranno N, Giraldi G, Sartori A, Gigli S, Barchetti G, *et al.* The role of 3 Tesla diffusion-weighted imaging in the differential diagnosis of benign versus malignant cervical lymph nodes in patients with head and neck squamous cell carcinoma. Biomed Res Int 2014;2014:532095.
14. Lee FK, King AD, Ma BB, Yeung DK. Dynamic contrast enhancement magnetic resonance imaging (DCE-MRI) for differential diagnosis in head and neck cancers. Eur J Radiol 2012;81:784-8.
15. Furukawa M, Parvathaneni U, Maravilla K, Richards TL, Anzai Y. Dynamic contrast-enhanced MR perfusion imaging of head and neck tumors at 3 Tesla. Head Neck 2013;35:923-9.
16. Xian J, Zhang Z, Wang Z, Li J, Yang B, Man F, *et al.* Value of MR imaging in the differentiation of benign and malignant orbital tumors in adults. Eur Radiol 2010;20:1692-702.
17. Yabuuchi H, Fukuya T, Tajima T, Hachitanda Y, Tomita K, Koga M. Salivary gland tumors: diagnostic value of gadolinium-enhanced dynamic MR imaging with histopathologic correlation. Radiology 2003;226:345-54.
18. Sasaki M, Sumi M, Kaneko K, Ishimaru K, Takahashi H, Nakamura T. Multiparametric MR imaging for differentiating between benign and malignant thyroid nodules: initial experience in 23 patients. J Magn Reson Imaging 2013;38:64-71.
19. Eida S, Sumi M, Nakamura T. Multiparametric magnetic resonance imaging for the differentiation between benign and malignant salivary gland tumors. J Magn Reson Imaging 2010;31:673-9.
20. Sumi M, Nakamura T. Head and neck tumours: Combined MRI assessment based on IVIM and TIC analyses for the differentiation of tumors of different histological types. Eur Radiol 2014;24:223-31.
21. Sasaki M, Sumi M, Eida S, Ichikawa Y, Sumi T, Yamada T, *et al.* Multiparametric MR imaging of sinonasal diseases: Time-signal intensity curve- and apparent diffusion coefficient-based differentiation between benign and malignant lesions. AJNR Am J Neuroradiol 2011;32:2154-9.
22. Wang YZ, Yang BT, Wang ZC, Song L, Xian JF. MR evaluation of sinonasal angiomatous polyp. AJNR Am J Neuroradiol 2012;33:767-72.
23. Yang BT, Li SP, Wang YZ, Dong JY, Wang ZC. Routine and dynamic MR imaging study of lobular capillary hemangioma of the nasal cavity with comparison to inverting papilloma. AJNR Am J Neuroradiol 2013;34:2202-7.
24. Driessen JP, Caldas-Magalhaes J, Janssen LM, Pameijer FA, Kooij N, Terhaard CH, *et al.* Diffusion-weighted MR imaging in laryngeal and hypopharyngeal carcinoma: association between apparent diffusion coefficient and histologic findings. Radiology 2014;272:456-63.
25. Habermann CR, Arndt C, Graessner J, Diestel L, Petersen KU, Reitmeier F, *et al.* Diffusion-weighted echo-planar MR imaging of primary parotid gland tumors: is a prediction of different histologic subtypes possible? AJNR Am J Neuroradiol 2009;30:591-6.
26. Vandecaveye V, De Keyzer F, Vander Poorten V, Dirix P, Verbeken E, Nuyts S, *et al.* Head and neck squamous cell carcinoma: Value of diffusion-weighted MR imaging for nodal staging. Radiology 2009;251:134-46.
27. Razek AA, Sieza S, Maha B. Assessment of nasal and paranasal sinus masses by diffusion-weighted MR imaging. J Neuroradiol 2009;36:206-11.
28. Wang X, Zhang Z, Chen Q, Li J, Xian J. Effectiveness of 3 T PROPELLER DUO diffusion-weighted MRI in differentiating sinonasal lymphomas and carcinomas. Clin Radiol 2014;69:1149-56.
29. Sakamoto J, Imaizumi A, Sasaki Y, Kamio T, Wakoh M, Otonari-Yamamoto M, *et al.* Comparison of accuracy of intravoxel incoherent motion and apparent diffusion coefficient techniques for predicting malignancy of head and neck tumors using half-Fourier single-shot turbo spin-echo diffusion-weighted imaging. Magn Reson Imaging 2014;32:860-6.

Received: 22-10-2014 **Edited by:** Xin Chen

How to cite this article: Wang XY, Yan F, Hao H, Wu JX, Chen QH, Xian JF. Improved Performance in Differentiating Benign from Malignant Sinonasal Tumors Using Diffusion-weighted Combined with Dynamic Contrast-enhanced Magnetic Resonance Imaging. Chin Med J 2015;128:586-92.

Source of Support: This work was supported by Beijing Excellent Talents Foundation (No. 2010D003034000033); Beijing Municipal Natural Science Foundation (No. 7112030), and high levels of health technical personnel in Beijing city (No. 2011-3-047). **Conflict of Interest:** None declared.